Received: 17 June 2024 | Revised: 27 August 2024 | Accepted: 19 September 2024

DOI: 10.1002/mp.17446

RESEARCH ARTICLE

MEDICAL PHYSICS

Assessing the biological effects of boron neutron capture therapy through cellular DNA damage repair model

Chenxi Yu[1] | **Changran Geng**[1,2,3] | **Xiaobin Tang**[1,2,3]

[1]Department of Nuclear Science and Technology, Nanjing University of Aeronautics and Astronautics, Nanjing, People's Republic of China

[2]Key Laboratory of Nuclear Technology Application and Radiation Protection in Aerospace, Nanjing University of Aeronautics and Astronautics, Ministry of Industry and Information Technology, Nanjing, People's Republic of China

[3]Joint International Research Laboratory on Advanced Particle Therapy, Nanjing University of Aeronautics and Astronautics, Nanjing, People's Republic of China

Correspondence
Changran Geng and Xiaobin Tang, Department of Nuclear Science and Technology, Nanjing University of Aeronautics and Astronautics, Nanjing, People's Republic of China.
Email: gengchr@nuaa.edu.cn and tangxiaobin@nuaa.edu.cn

Funding information
National Key Research and Development Program, Grant/Award Number: 2023YFE0197700; National Natural Science Foundation of China, Grant/Award Number: 12261131621; Natural Science Foundation of Jiangsu Province, Grant/Award Number: BK20220132

Abstract

Background: Boron neutron capture therapy (BNCT) is a targeted radiotherapy that relies on the ^{10}B (n, α) ^{7}Li reaction, which produces secondary particles with high linear energy transfer (LET), leading to a high relative biological effectiveness (RBE) in tumors. The biological effectiveness of BNCT is influenced by factors such as boron distribution and concentration, necessitating improved methods for assessing its radiobiological effects and clarifying the sensitivity of the differences in different factors to the biological effects.

Purpose: This paper introduces a method to evaluate the biological effects of BNCT using the cellular repair model. This method aims to overcome some of the limitations of current evaluation approaches. The primary goal is to provide guidance for clinical treatments and the development of boron drugs, as well as to investigate the impact of the synergistic effects of mixed radiation fields in BNCT on treatment outcomes.

Methods: The approach involves three key steps: first, extending the radial energy deposition distribution of BNCT secondary particles using Geant4-DNA. This allows for the calculation of initial DNA double-strand breaks (DSBs) distributions for a given absorbed dose. Next, the obtained initial DSB distributions are used for DNA damage repair simulations to generate cell survival curves, then thereby quantifying RBE and compound biological effectiveness (CBE). The study also explores the synergistic effects of the mixed radiation fields in BNCT on assessing biological effects were also explored in depth.

Results: The results showed that the RBE of boronophenylalanine (BPA) and sodium borocaptate (BSH) drugs at cell survival fraction 0.01 was 2.50 and 2.15, respectively. The CBE of the boron dose component was 3.60 and 0.73, respectively, and the RBE of the proton component was 3.21, demonstrating that BPA has a significantly higher biological impact than BSH due to superior cellular permeability. The proton dose significance in BNCT treatment is also underscored, necessitating consideration in both experimental and clinical contexts. The study demonstrates that synergistic effects between disparate radiation fields lead to increased misrepairs and enhanced biological impact. Additionally, the biological effect diminishes with rising boron concentration, emphasizing the need to account for intercellular DNA damage heterogeneity.

Conclusions: This methodology offers valuable insights for the development of new boron compounds and precise assessment of bio-weighted doses in clinical settings and can be adapted to other therapeutic modalities.

KEYWORDS
boron neutron capture therapy, DNA damage repair model, relative biological effectiveness, synergistic effects

1 | INTRODUCTION

Boron neutron capture therapy (BNCT) is a tumor treatment that theoretically targets malignant cells while sparing normal cells. It relies on the nuclear capture reaction between low energy thermal neutrons and ^{10}B, producing highly linear energy transferring (LET) α and ^{7}Li that can precisely kill tumor cells due to their short range.[1] In addition to the α and ^{7}Li ions produced by the boron capture reaction $^{10}B(n,\alpha)^{7}Li$, the main dose components are the photon dose from the $^{1}H(n,\gamma)^{2}H$ reaction and the nitrogen dose from the 0.58 MeV protons produced by the $^{14}N(n,p)^{14}C$, the hydrogen dose from the recoil protons produced by the $^{1}H(n,n)p$ reaction.[2] The relative biological effectiveness (RBE) of the boron dose component is usually described by the compound biological effectiveness (CBE), which combines the effects of α and ^{7}Li and is influenced by factors such as boron distributions.[3] Considering the differences in these factors, it is important to study the biological effects of BNCT. There have been many experimental studies on the biological effects of BNCT as early as the twentieth century[4–6]; however, the results obtained from different experimental conditions are widely disparate and there are uncertainties in the experimental methods. There have also been studies using simulation methods to predict biological effects. For example, Han et al. and Nakano et al. developed and applied a series of methods to explore the RBE of different types of radiation by predicting the physical differences in the yield and distribution of DSB from initial DNA damage.[7,8] However, physical differences in DNA damage are only the first stage of the biological effects of radiation, these initial damages are subsequently dealt with by a series of cellular repair processes, and the ability of cells to detect, repair and respond to these damages is critical in determining their radiosensitivity. Frankenberg has demonstrated that biological endpoints such as chromosomal aberrations, cell death, oncogenic cell transformations and gene mutations occur after cellular damage repair, particularly at low doses, with much higher RBE values than those estimated based solely on initial DSB.[9] Therefore, it is crucial to explore bioremediation models that encompass a variety of repair pathways and molecular mechanisms.

Several cellular repair models have been developed and applied to predict cellular DNA damage repair, such as those of Warmenhoven et al., McMahon et al., and Belov et al.[10–12] The predictions of these models in terms of cellular repair kinetics reproduce the experimental results well. There are also examples of integrating cell repair models into programs to directly predict cell survival fraction in Geant4-DNA.[13] However, the mechanisms of repair in BNCT are not well understood,[14] and there are no studies applying the cell repair mechanism to BNCT to investigate the biological effects. Furthermore, there are synergistic effects in the radiation field of different ray types in BNCT.[15,16] For example, Guerra Liberal et al. investigated the synergistic effects of high LET and low LET radiation, and showed that the combination of different radiation qualities produces unexpected synergistic effects, which should be taken into account in treatment design.[17] A new model to estimate the biological effects of BNCT was developed by Sato et al., the effect of this synergistic effects was taken into account in their model, and the effect of synergistic effects on the final RBE of BNCT treatment was also demonstrated.[2] However, the mechanism of action of the synergistic effects on DNA damage repair in BNCT is not yet fully understood, and further investigation is necessary.

In this work, the biological effects of BNCT were explored using the Mechanistic DNA Repair and Survival Model (Medras)[11] cellular repair model proposed by McMahon et al., which simulates the repair of radiation-induced DNA damage, incorporating the overall kinetics of repair and its fidelity to predict a range of biological endpoints. The model was not applied to the low-energy particles produced by BNCT; therefore, this work extends its application to BNCT, using the commonly used clinical treatment drugs BPA and BSH as research subjects.

The specific calculations are shown below, and the biological effects calculated by this approach are compared with the corresponding experimental data. Finally, the effects of different boron drug distributions and different boron drug concentrations on the cell survival fraction (SF) are discussed as a means of estimating the RBE and CBE of the different dose components. Additionally, this study delves deeper into the effects of synergistic interactions on the SF in the BNCT radiation field.

2 | METHODS

2.1 | DNA damage and repair simulation using Medras

The Medras cellular repair model simulates the repair of radiation-induced DNA damage by integrating overall repair kinetics and fidelity, enabling the prediction of various biological endpoints. The model begins with the distribution of double-strand breaks (DSBs), tracks the repair progress, and assesses the distribution of misrepaired DSBs. Biological endpoints, including the quantification of unrepaired and misrepaired DSBs, mutations, and chromosome aberrations, are then used to estimate cell survival probability.[11] DSBs can be repaired by one of three pathways, Nonhomologous End Joining, Homologous Recombination, and Microhomology Mediated End Joining, which correlate with cell

cycle phase and pathway activity.[18–20] Medras models all of these repair pathways in a two-step process, whereby firstly each DSB initially consists of two free ends and physically interacts with nearby free ends at a rate related to the complexity of the breaks and their initial distribution. Pairs of free breaks can join together to restore DNA structure, after this point, the DSB ends will not be able to recombine with other broken ends. Both stages in repair are modeled as simple exponential processes in Medras.

In the Monte Carlo version of Medras, DSB distributions are efficiently generated for various particle types and energies by calculating radial energy deposition within cells.[11] This method estimates the number of DSB around an ion track at a radial distance r based on energy deposition $E(r)$ and an average energy threshold (E_{DSB} = 56.5 keV) required for DSB induction. The resulting initial DSB distribution is output in the DNA damage standard file format.[21] After generating the initial distribution of DSB, Medras reads this information to obtain details such as break complexity and spatial characteristics. It calculates the interaction rate ($\zeta_{i,j}$) of each endpoint of the break and the total rate(η_i) between free endpoints. The effective rate (λ_i) for each break is then derived from the total interaction rate, as described in Equation (1).

$$\lambda_i = \lambda_x \eta_i \tag{1}$$

In Equation (2), the repair time (t_i) associated with each break endpoint is randomly sampled using a uniformly distributed random variable X between 0 and 1. Simulations then proceed by repairing endpoints starting from the one with the smallest t_i, with subsequent endpoints repaired based on their increasing repair times.

$$t_i = -\frac{\log(X)}{\lambda_i} \tag{2}$$

During simulation, a free endpoint is randomly chosen from all remaining endpoints based on the $\zeta_{i,j}$. This pair of free endpoints is then removed from the simulation after recording it as a repair event, and values such as h_i and t_i are updated for all remaining breaks. The process is then repeated for the next smallest t_i until all broken endpoints have been reconnected.

Cell survival at specific doses was analyzed using Medras to study misrepair events caused by radiation exposure. This analysis included quantifying remaining breaks, misrepaired breaks, "large" misrepairs, and interchromosomal misrepairs to assess the probability of cell survival post-irradiation.[11] The cell survival probabilities of the three different dose components—namely the boron dose(caused by α and ^{7}Li), the proton dose (including nitrogen dose and the hydrogen dose), and the photon dose were calculated and fitted the cell survival curves using a linear quadratic model (LQ model).[22]

2.2 | Cell survival curve calculation for BNCT situations

Figure 1 shows the flowchart of the calculations. Medras does not include the radial energy deposition of low-energy protons, α, and ^{7}Li. Therefore, this study first utilizes Geant4-DNA to calculate the radial energy deposition of secondary particles at BNCT energies and applies this to Medras to calculate the initial distribution of DSBs for the corresponding doses in BNCT.

In addition to the energy deposition of particles at corresponding energies, Medras requires the dose deposited by these particles within the cell nucleus to generate DNA damage distributions. Therefore, it is necessary to obtain the dose deposited by particles of different energies in the cell nucleus. The detailed dose calculation process for each energy particle is shown in Part 2 of Figure 1. For tumor cells, the main dose in BNCT is generated by α and ^{7}Li produced by ^{10}B (n, α) ^{7}Li. However, these particles have a short range of about 5–9 μm, leading to a discrepancy between the intranuclear dose and the macroscopic absorbed dose. To address this, a dose factor $F_{i,j}$ needs to be calculated. Where i represents the BNCT secondary particle type, and j represents the microscopic distribution of different boron drugs (e.g., BPA and BSH). After obtaining the dose factor $F_{i,j}$, the intranuclear doses of α and ^{7}Li can be calculated according to Equation (3) for different boron drug distributions at a given macroscopic absorbed dose.

$$D_{i,j} = D_{abosrbed} \times F_{i,j} \tag{3}$$

The initial energies of α and ^{7}Li produced by BNCT are fixed, but their energies vary when reaching the cell nucleus due to different starting positions. Medras requires these particles at the nucleus membrane to be treated as initial particles, with their corresponding nucleus doses provided to generate the DNA damage distribution. Therefore, the contributions of particles with different energies reaching the nucleus membrane to the nucleus dose must also be calculated. This is calculated with Equation (4)

$$D_{i,j,k} = \sum_{m=1}^{4} D_{i,j} \times W_{i,j,m} \times P_{i,j,m,k} \tag{4}$$

where W represents the contributions to the dose absorbed in the nucleus due to particles starting at different initial positions. The meanings represented by

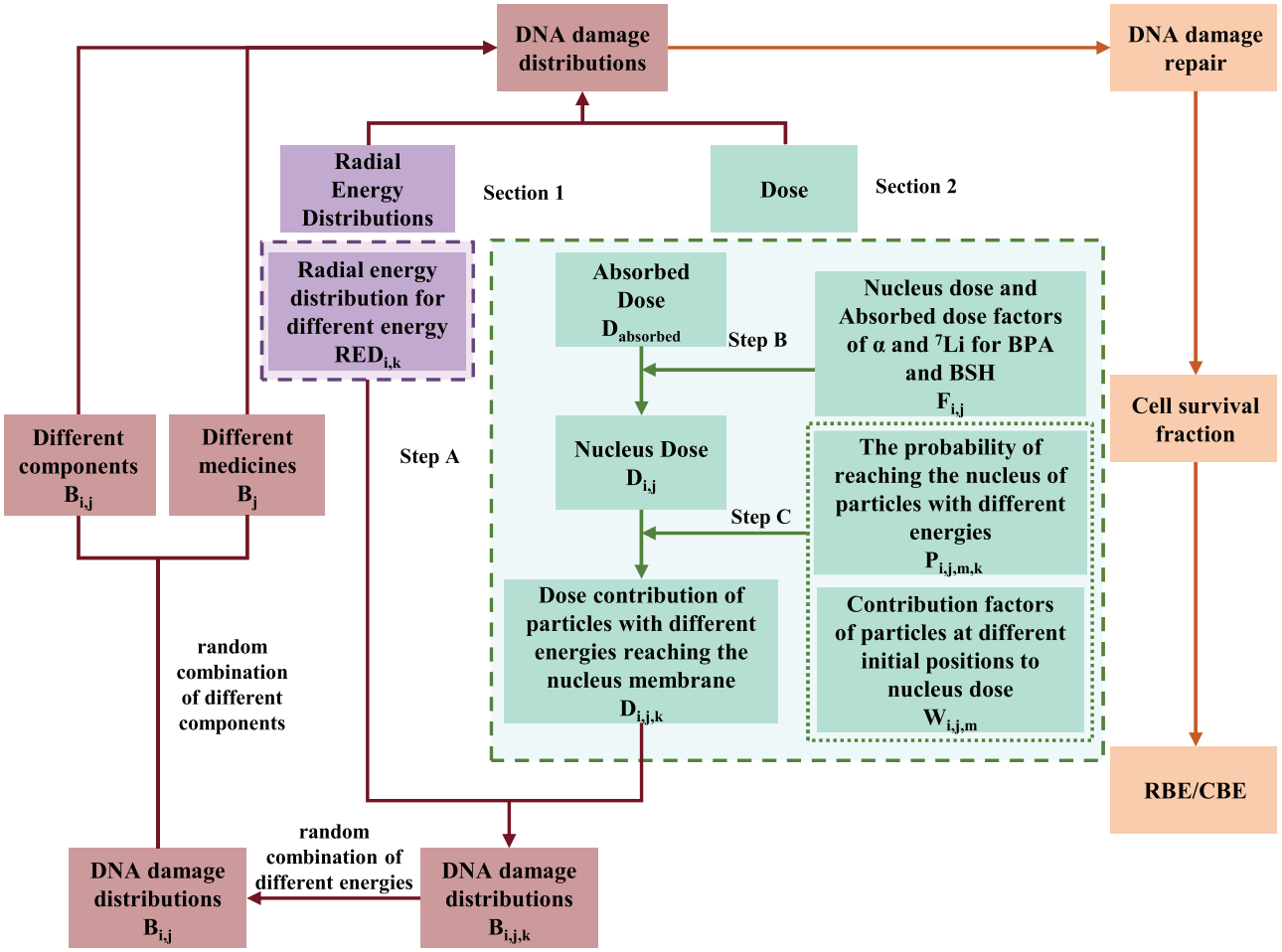

FIGURE 1 Overall workflow diagram.

i and *j* are the same as Equation (3). The variable *m* represents the different boron drug distribution locations, include nucleus ($m = n$), the cytoplasm($m = c$), the cell membrane ($m = s$), and the extracellular ($m = e$). Since BPA can enter the cell via the amino acid transporter,[23,24] it is assumed to be distributed in the cytoplasm and extracellular space, but not in the nucleus. BSH have both cell membrane and extracellular distributions because BSH cannot cross the cell membrane.[25] *k* represents different energies of particles. For α, $k = 0.2, 0.4 \ldots 1.2, 1.47, 1.78$ MeV, and for ^{7}Li, $k = 0.2, 0.4, 0.6, 0.84, 1.02$ MeV. *P* is the probability density integral of different energies of *k* under different boron drug distribution locations obtained from our previous work.[7]

With these parameters, the initial DNA damage distribution of different energy secondary particles under different drug distributions was obtained. The DNA damage caused by particles with different energies was then randomly combined to obtain the final DNA damage for different particles under various drug distributions. The DNA damage produced by α and ^{7}Li was combined as the DNA damage from the boron dose, while the DNA damage from recoil protons and 0.58 MeV protons was combined as the DNA damage from the proton dose. The DNA damage produced by all particles was randomly combined as the DNA damage produced at the total dose, where the mixing of DNA damage from different dose components was considered as synergistic effects. These were read using Medras for cellular DNA damage and repair simulations.

2.3 | Detailed steps to calculate the parameters in the model

2.3.1 | Step A: Radial energy deposition calculation

Only DNA damage distributions for monoenergetic particles can be generated in Medras, whereas the energies at which α and ^{7}Li in BNCT reach the cell nucleus after traversing different distances have a probability distribution. This probability was calculated

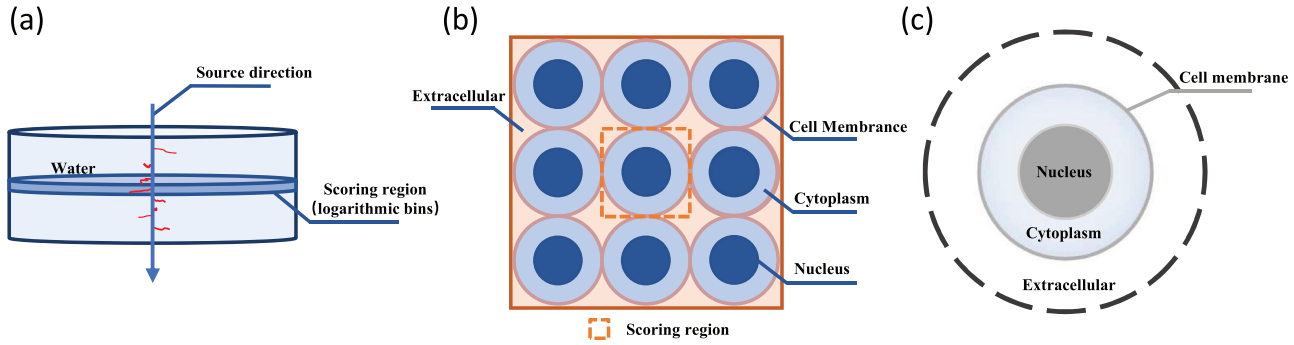

FIGURE 2 The geometrical model: (a) schematic diagram of radial energy deposition modeling for Geant4-DNA calculations in step A. (b) The cell modeling cross-sections in TOPAS-nBio in step B, (c) the cell modeling cross-sections in TOPAS-nBio in step C.

in previous studies.[7] Therefore, in this work, the radial energy deposition of BNCT secondary α and ^{7}Li with different energies when they reach the nucleus, as well as the radial energy deposition of recoiling protons with probability distributions of energies mainly in the range of 0.001–1 MeV, is simulated.

To calculate radial energy deposition, the open-source Geant4-DNA Monte Carlo toolkit is used for modeling.[26,27] Figure 2a shows the geometrical model obtained with Geant4. Ions of various species and energies are emitted towards the center of a cylindrical water phantom with a radius of 200 μm and a depth of 22 μm. The energy deposition of primary ions and secondary electrons is recorded at the center depth and scored according to the radial distance to the primary particle trajectory when entering the recording region. To minimize the effect of scattering from low-energy particles, the thickness of the counting region is set to 0.5 μm, and the particle source is placed at the center of the counting region surface. For the physical model, the physical process G4EmDNAPhysics in Geant4-DNA is selected.

2.3.2 | Step B: Calculation of nuclear and cellular absorbed dose factors

The TOPAS-nBio Monte Carlo toolkit[28] is used to calculate the F factor. In TOPAS-nBio, a geometrical model of a 3 × 3 × 3 cell nucleus is constructed, as shown in Figure 2b, with a nucleus radius of 4.32 μm and a cell radius of 8 μm. The particle source needs to be set up according to the different boron drug microdistributions and the permeability of different drugs. The boron element ratio N represents the percentage of ^{10}B atoms relative to the total number of ^{10}B atoms at different locations, $n, c, s,$ and e are used to represent the nucleus, the cytoplasm, the cell membrane, and the extracellular, respectively, and the formula is shown in Equation (5)

$$\frac{N_n + N_c + N_s}{V_{cell}} : \frac{N_e}{V_{Ec}} = C_B \tag{5}$$

where V_{cell} represents the cell volume and V_{Ec} represents the extracellular volume within a region. For BPA, $N_n = Ns = 0$, and for BSH, $N_n = N_c = 0$. The reference boron concentration ratio C_B in this study was taken from the experimental data of melanoma cells with BPA about 3.2, and BSH about 0.86[2]. N_c and N_e are 0.78 and 0.22 for BPA, and N_s and N_e are 0.48 and 0.52 for BSH, respectively. The ratio of the dose to the nucleus in the scoring region (located in the center of the geometry) to the dose in the scoring region is F.

2.3.3 | Step C: Calculation of nuclear dose contribution factors for particles at different locations

The TOPAS-nBio Monte Carlo toolkit[28] was used also to obtain the W factor. The geometry was built as shown in Figure 2c, but here the situation was simulated separately when the particle source was located at different emission positions. In this work, the contribution of extracellular and cytoplasmic α and ^{7}Li to the nucleus dose of the BPA drug, and the contribution of extracellular and cell membrane α to the nucleus of the BSH drug were calculated separately, for the BSH drug, the contribution of the ^{7}Li to the nucleus dose was not take into account, because the ^{7}Li, which is distributed in the cell membrane and the extracellular, hardly reaches the nucleus in this model.

2.4 | Evaluating the synergistic effects of BNCT mix radiation conditions

To investigate the effect of the synergistic effects on cell repair, the DNA damage distributions from each dose component of BNCT were combined based on their respective contributions. This combination represents the DNA damage distribution caused by different radiation fields. In this work, only the spatial distribution of DNA damage is considered, without accounting for temporal distribution or dose rate effects. Cell repair

simulations were conducted using the mixed DNA damage distribution, cell survival probabilities under varying total absorbed doses were calculated, and the LQ model was used to fit the cell survival curve. The survival probability of each dose component was accumulated based on the LQ model. The accumulation formula is shown in Equation (6), which represents the cell survival curve under the total absorbed doses without considering the synergistic effects.

$$-\ln(S(D_{mix})) = \sum_{i=1}^{3} (\alpha_i D_i + \beta_i D_i^2) \quad (6)$$

where $D_{mix} = \sum_{i=1}^{3} D_i$, represents the total absorbed dose. D_1, D_2, and D_3 represent the doses of the different dose components of BNCT (boron dose, proton dose, and photon dose), respectively, and D_1: D_2: D_3 follows the dose share of the different dose components in BNCT treatment. In the LQ model, the β term represents the "multiple-hit" cell death caused by the interaction of damage from different radiation tracks.[22] It only considers the incoherent action of two independent events that produce damage entities but does not include cross terms. Moreover, in the direct accumulation shown in Equation (6), this approach fails to capture the synergistic effects between different types of radiation. In the photon iso-effective dose model proposed by Gonza´lez et al.,[29] the synergistic effects between different types of radiation are considered. To compare the results of the simulations with the cell survival curves obtained with and without considering synergistic effects, the photon iso-effective dose model is used. In the photon iso-effective dose model considering synergistic effects, an assumption was that the time-dependent factor remains constant.

3 | RESULT

3.1 | Radial energy deposition of BNCT secondary particles

Figure 3 presents the radial energy deposition, energy deposition rate per counting region, and cumulative radial energy deposition rate for α, ^{7}Li, and protons involved in BNCT. Calculations of high-energy protons and α were compared with previous work by McMahon et al.,[11] showing differences within 1 nm. Specifically, the calculations deposit more energy within a radial distance of $r = 0.1$ nm, less energy between 0.1 and 1 nm, and show better agreement beyond 1 nm, resulting in overall consistent total deposited energy. These variations may stem from nuances in Monte Carlo scoring, including the Geant4 version and cross-section used. However, the energy deposition around the 1 nm radial track in the Medras repair model has no measurable effect on the repair results.

The repair results of cells under 1 Gy proton and α irradiation with different LETs in Medras, as calculated in this work, are compared with the results calculated by McMahon et al.[11] The absolute errors in cell survival rates are all less than 0.05, which is within a reasonable range.

3.2 | DNA damage distribution

In this study, the clinically utilized boron drugs BPA and BSH were investigated, and calculated the dose factors for each of these drugs. In the cellular model, the calculated results are $F_{\alpha,BPA} = 0.85$, $F_{Li,BPA} = 0.41$, and $W_{\alpha,BPA,c} = 0.98$, $W_{\alpha,BPA,e} = 0.02$ for BPA. For the BSH, the calculated results are $F_{\alpha,BSH} = 0.29$, $F_{Li,BSH} = 0$, $W_{\alpha,BSH,c} = 0.42$, $W_{\alpha,BSH,e} = 0.58$. These ratios reflect how boron drug characteristics influence the distribution of secondary particles within cellular structures, affecting the effectiveness of radiation delivery to target areas. It should be emphasized that these two dose factors correlate with the nucleus and cell size, and the nucleus size selected in this study is consistent with typical estimates of nucleus radius.

Based on the obtained radial energy deposition and the corresponding doses of various particles, the misrepair classification was obtained under the DNA damage distribution of different dose components of boron drugs, as shown in Figure 4a.

Figure 4b shows the direct accumulation of misrepairs under different radiation fields and the misrepairs under the total radiation field, the diagonal-striped group is the repair results of the total dose, and the blank group is the direct accumulation of each dose component. The error of Dicentric Aberrations, Rings Aberrations, and Total Aberrations is too small and the error bar is not shown in the figure. The data reveal that combining DNA damage distributions from diverse radiation fields leads to a greater overall misrepair count compared to the sum of misrepairs from individual radiation fields. Furthermore, conspicuous disparities in misrepairs are evident between chromosomes.

3.3 | Prediction of survival curves under BNCT secondary particle irradiation

To verify whether the DNA damage distribution obtained by this method can be used to predict the cell survival fraction in the subsequent cell repair model, several DNA damage distributions were generated under gamma, proton, and alpha rays and used to simulate repair respectively, the obtained cell survival curve are compared with experimental values.

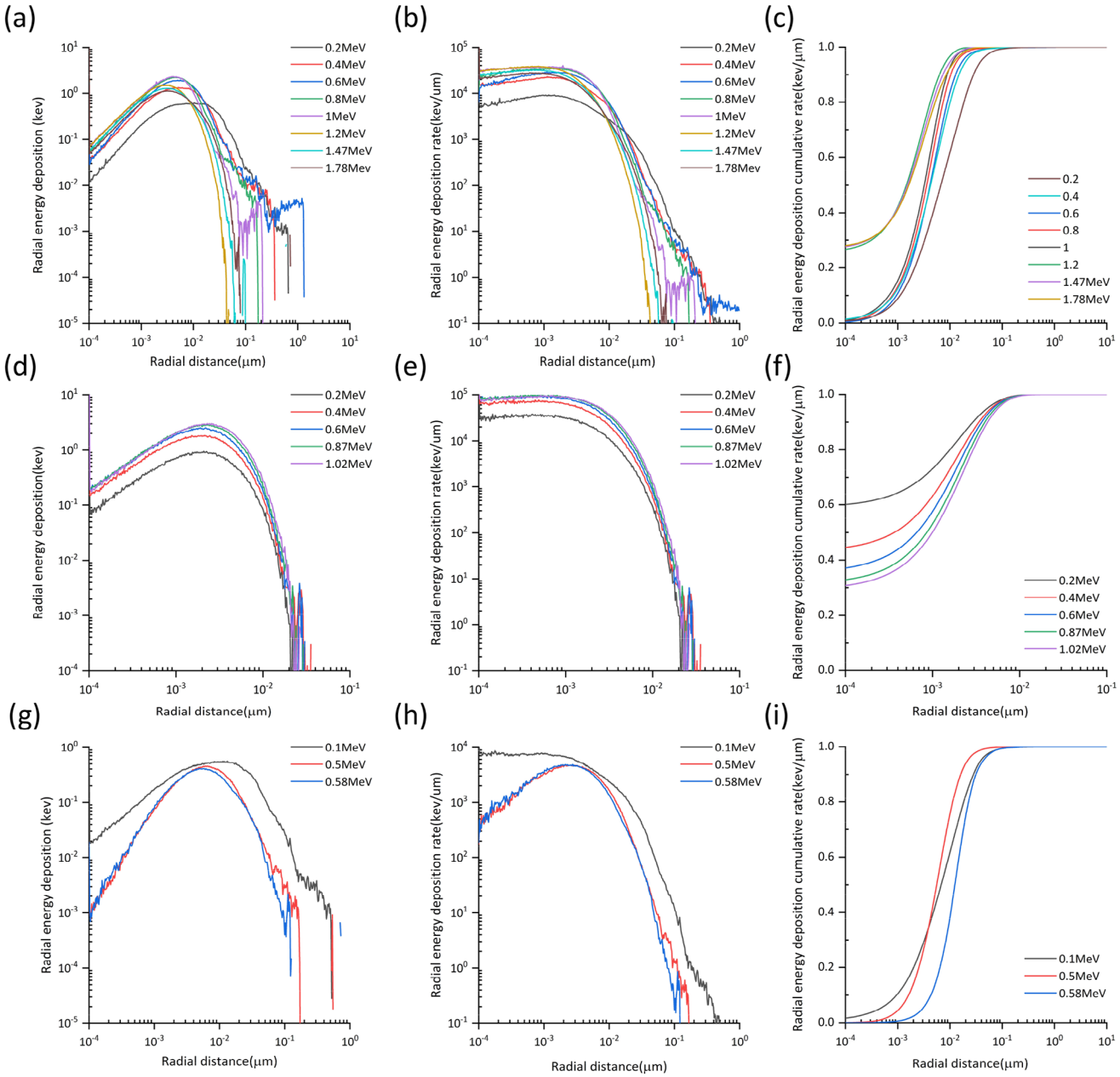

FIGURE 3 Radial energy deposition, energy deposition rate per counting region, and cumulative radial energy deposition rate of different energy particles that can reach the surface of the nucleus by the BNCT reaction. (a–c) α, (d–f) ^{7}Li, (g–i) proton.

Figure 5 shows the predicted cell survival curves under ^{60}Co-γ source, ^{210}Po-α source, and proton source, respectively, with experimental data of different cell lines.[30–35] Figure 6 shows the simulation curves of cell repair kinetics at different doses of different types of irradiation in comparison with experimental results,[36–40] which can also reflect the trend of DSB repair over time.

The results show that the repair result predicted by the Medras can be adapted to a range of cell lines, and although it is not representative of any cell line, it can better reflect a trend of the survival fraction of human cells in relation to the dose.

3.4 | Cell survival curves under different dose components and total dose field

In this work, the cell survival fraction of each dose component in the BNCT radiation field was first simulated to obtain the corresponding RBE (CBE), and then simulated cell survival for different boron drug micro distributions, that is, comparing two drugs, BPA and BSH. Additionally, cell survival was simulated for different boron drug concentrations.

Figure 7a presents Medras-predicted cell survival fraction of BNCT different dose components plotted

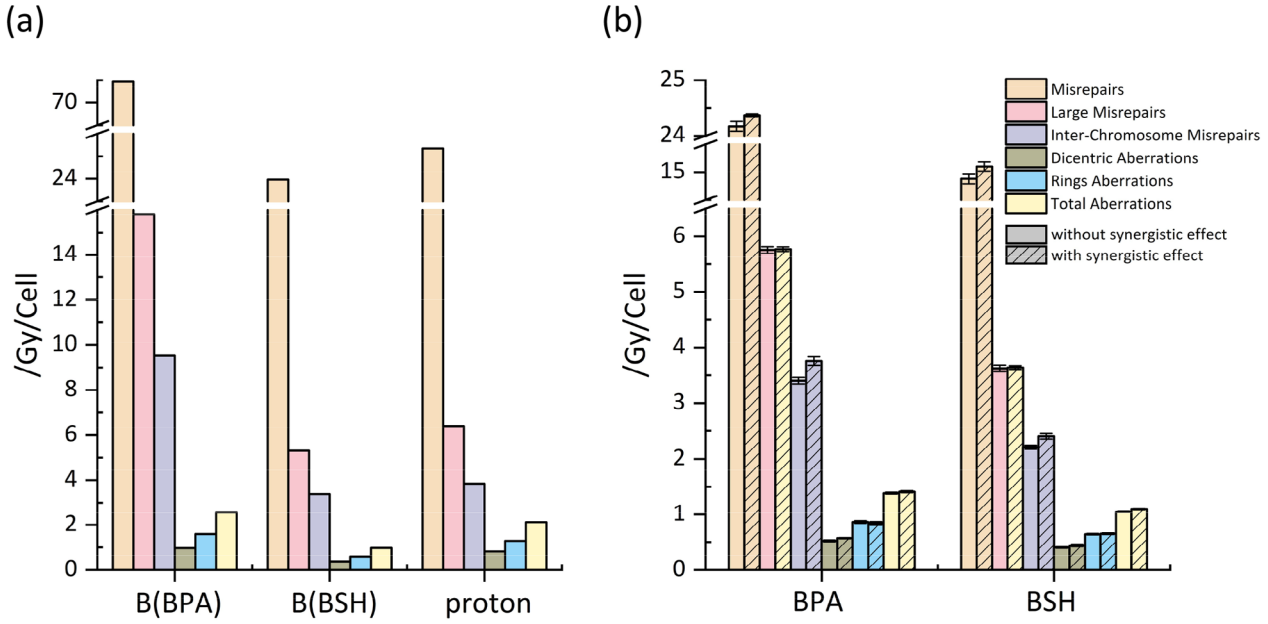

FIGURE 4 Misrepairs classification. (a) Misrepairs classification from different dose components of boron drugs. (b) Misrepairs classification with (blank) and without (diagonal-striped) considering synergistic effects.

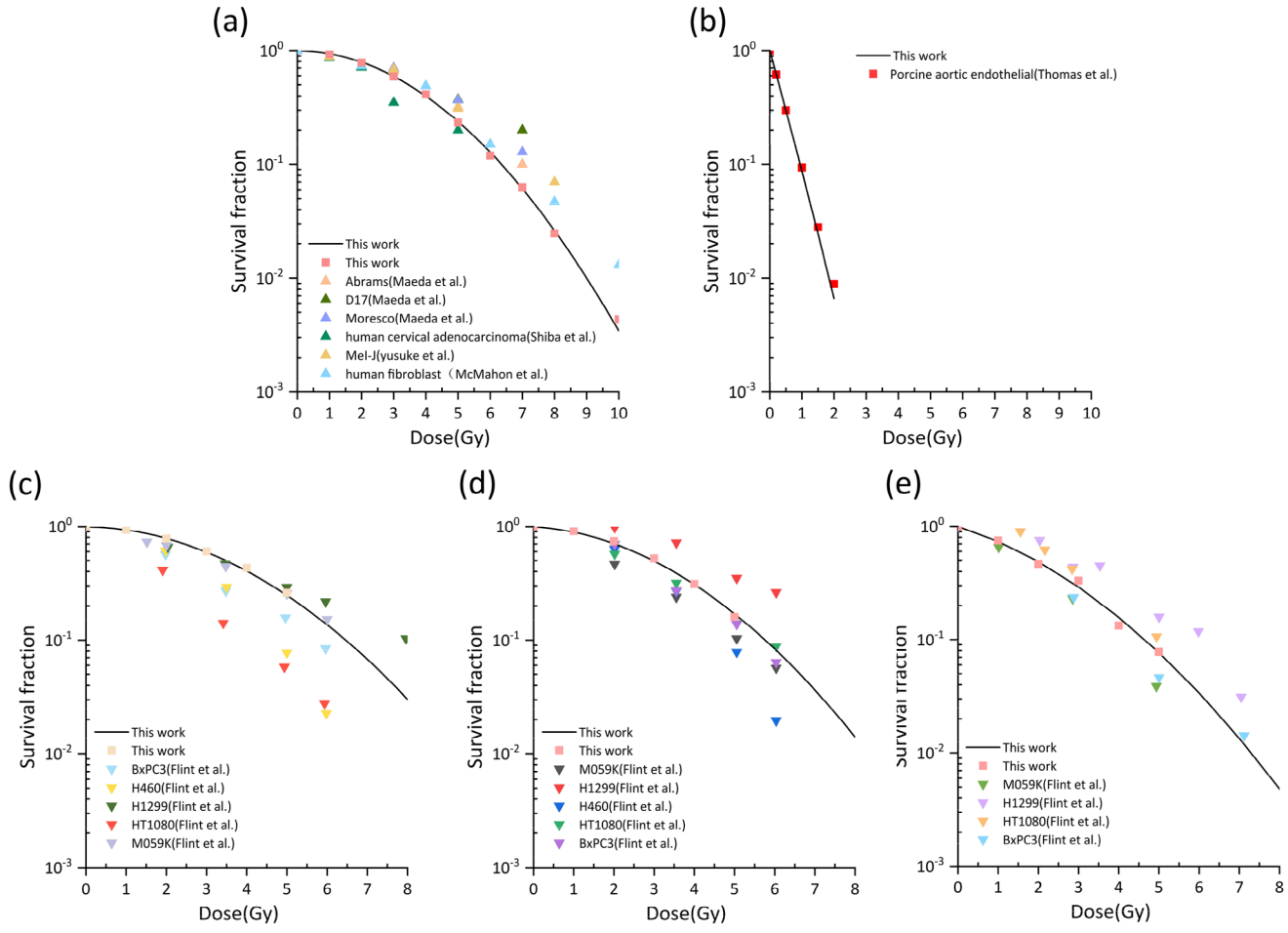

FIGURE 5 Comparison of predicted survival curves of different types of ray-derived cells with experimental data from different cell lines. (a) Photon, (b) alpha, (c–e) proton.

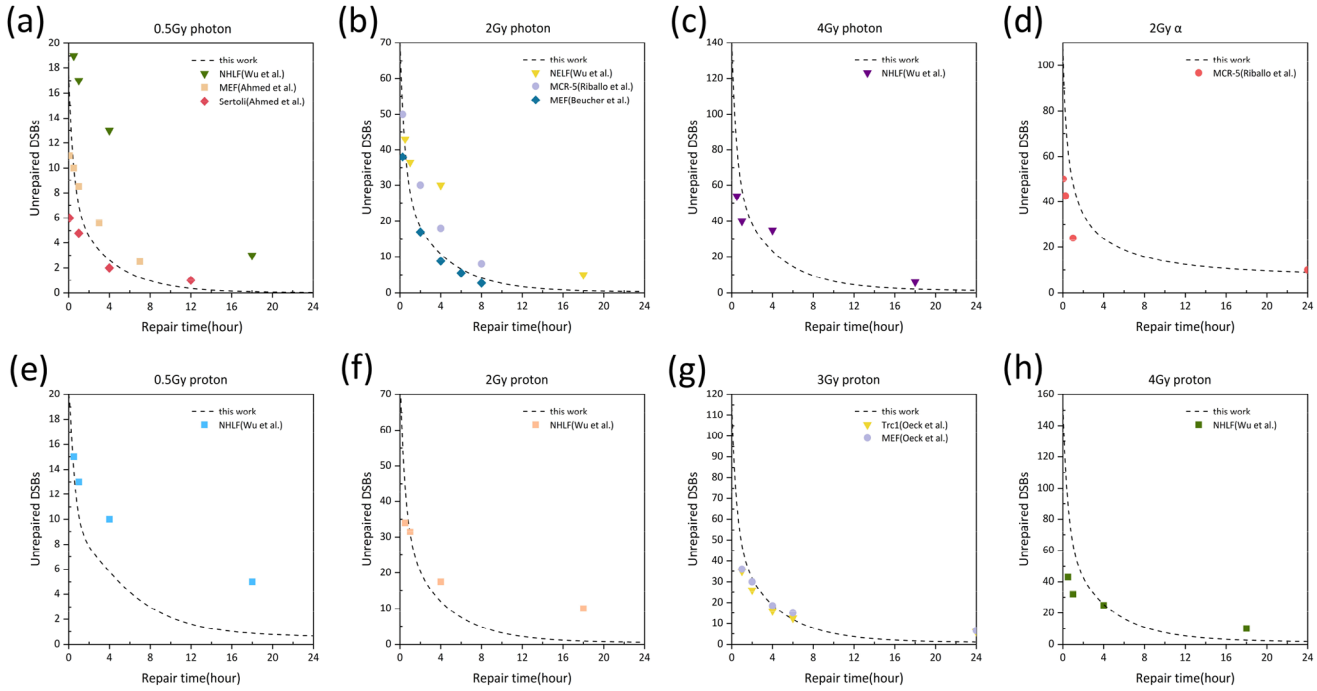

FIGURE 6 Simulation curves of cell repair kinetics at different doses compared with experimental results, (a–c) photon, (d) alpha, (e, f) proton.

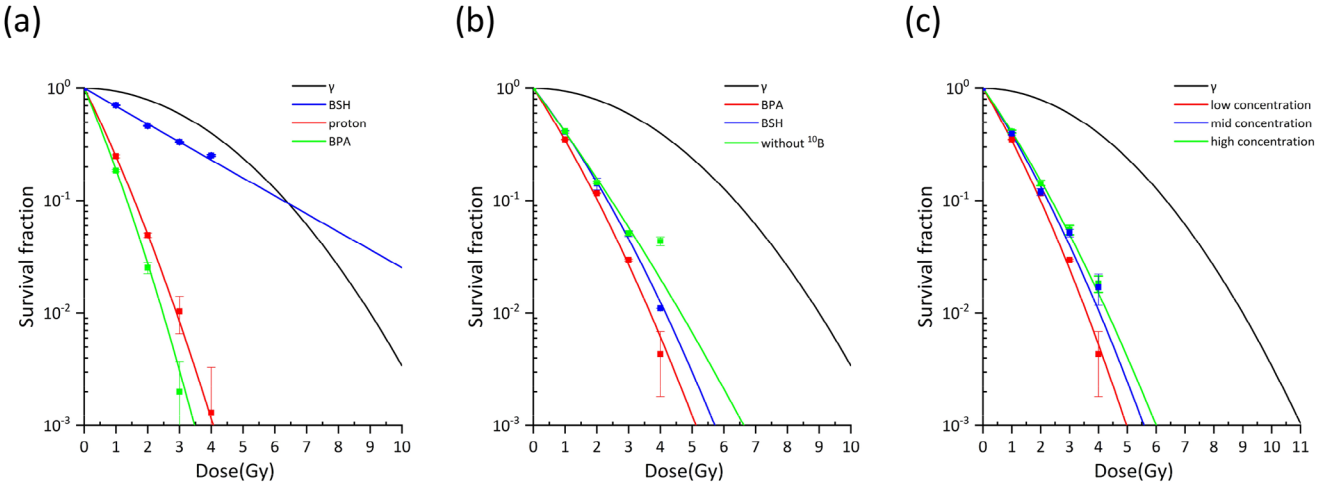

FIGURE 7 (a) Predicted cell survival curves obtained for different BNCT dose component, (b) cell survival curves of BPA and BSH drugs after considering synergistic effects, (c) cell survival curves of BPA drugs at three boron dose contribution.

against the dose. The data points indicate cell survival fractions at specific absorbed doses, with fitted curves based on the LQ model. Notably, the CBE of the BPA drug's boron dose component exceeds that of the BSH drug, while the proton dose component exhibits intermediate RBE. Figure 7b illustrates the cell survival fraction of the BPA and BSH drugs, plotted as a function of the total absorbed dose of the boron-containing components in the tumor.

3.5 | RBE and CBE

Table 1 summarizes the comparison of the RBE (CBE) at different survival fractions under various dose components and different boron drug distributions with previous literature. It can be seen that the use of cell repair models can predict effectively the RBE (CBE) of BNCT.

The impact of different boron concentrations of BPA on the effectiveness of BNCT treatment was also

TABLE 1 Comparison of RBE (CBE) at different survival fractions for each dose component and total at different boron drug distributions with previous literature.

Component	RBE_{50}	RBE_{10}	RBE_1	Experimental	Reference
γ	1	1	1	1	–
Proton	6.87	3.97	3.21	3.2[b]	6
B (BPA)	7.34	4.70	3.60	5.65[a]	41
				3.8[b]	6
B (BSH)	1.94	1.02	0.73	2.29[a]	41
				1.2[b]	6
Total	**RBE_{50}**	**RBE_{10}**	**RBE_1**	**Experimental**	**Reference**
BPA	5.18	3.20	2.50	2.52[c]	4
				2.81[b]	2
BSH	4.64	2.67	2.15	1.99[b]	2
Without B	4.65	2.56	1.95	1.99[c]	4
				1.25[b]	2

[a]The biological endpoint chosen was D0 ratio (SF = 0.37).
[b]The biological endpoint chosen was SF = 0.01.
[c]The biological endpoint chosen was growth delay time.

considered in this work. Different boron concentrations correspond to varying dose proportions: at low concentration, boron accounts for 20%, with protons and γ-rays each accounting for 40%; at medium concentration, boron accounts for 45%, with protons at 27% and γ-rays at 28%; at high concentration, boron accounts for 65%, with protons at 17% and γ-rays at 18%. Boron concentrations were selected based on experimental data.[4] Figure 7c shows the cell survival curves of BPA drugs at three boron dose occupancies. Based on the results, it appears that as the boron concentration increases, its biological effect decreases.

3.6 | Synergistic effects

Figure 8 shows the effect of synergistic effects on the different drugs of BNCT and the comparison with the photon iso-effective dose model. The solid line represents the results considering synergistic effects, while the dashed line represents the results without considering synergistic effects. Different colors correspond to the cell survival curves predicted by this study and the cell survival curves calculated by the equivalent photon model. The results show that the cell survival fraction for the same dose is smaller when the synergistic effects is taken into account, which confirms that there is indeed some synergistic effects of BNCT. The effect of synergistic effects needs to be considered when using the concept of CBE in the clinic. This approach of considering the synergistic effects of the BNCT radiation field is also further validated by comparison with the photon iso-effective dose model.

4 | DISCUSSION

BNCT is a treatment method for malignant tumors. In clinical practice, it is typically assumed that RBE (CBE) value of BNCT is constant. However, in reality, this value can be influenced by factors such as the distribution of boron drugs. Therefore, studying the biological effects of BNCT is of significant importance. This work proposes a method to evaluate the RBE (CBE) of BNCT based on cellular DNA damage repair mechanisms.

To validate the feasibility of this method, the application of the Medras cellular repair model was extended to BNCT secondary particles. Subsequently, simulations of cell survival rates and DNA damage repair kinetics for different radiation types in BNCT at corresponding energies and doses were conducted to verify the model's predictive effectiveness. The results show that the predicted values of the Medras model in terms of cell survival probability and repair kinetics match well with the overall trend of the experimental dataset.[30,40] The findings show consistency across different cell lines, whereas the same type of cell line may exhibit significant differences due to experimental conditions and other factors. Therefore, the findings represent a trend across multiple cell lines rather than replicating results for a specific cell line.

This work also simulated the cell survival curves for different dose components and total dose fields of the drugs BPA and BSH, and quantified the RBE (CBE). The predicted results for a 1% cell survival rate as the biological endpoint were similar to the experimental results. Notably, the RBE values varied significantly depending on the choice of cell survival rates, with higher cell survival rates associated with higher RBE values. This indicates the need to consider the choice of biological endpoints when calculating the RBE. Additionally, it was found that the CBE of BPA was significantly higher than the biological effects of BSH, which was due to the difference in the distribution of the boron drug resulting from the varying permeability of the cells to the two drugs, BPA can enter the cells and distribute in the cytoplasm so that the same macroscopic dose can reach the nucleus of the cell with a greater number of α and ^{7}Li leading to the production of more DSBs. The results also show that the biological effects of proton dose in BNCT treatment cannot be ignored. This suggests that both in experimental and clinical settings, it may be necessary to consider the proton dose of the beam and its impact on the RBE.

The biological effects, with and without considering synergistic effects, were compared. Although temporal effects were not considered in this work, the results (Figure 8) suggest that when synergistic effects are taken into account, the spatial co-action of different types of rays produces synergistic effects, resulting in

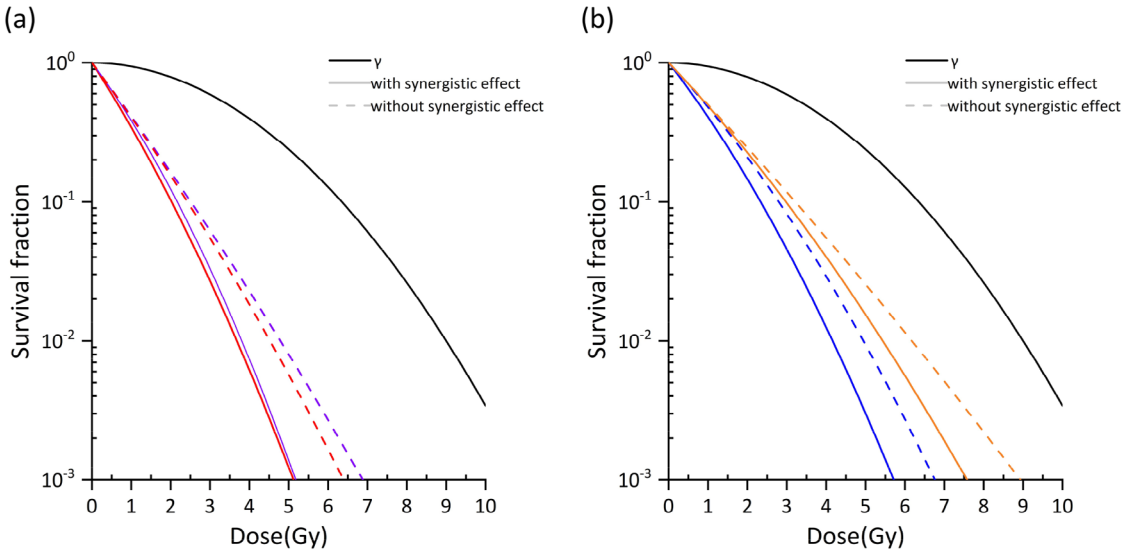

FIGURE 8 Effect of synergistic effects on different drugs of BNCT in this work and comparison with photon iso-effective dose model. (a) For BPA distribution: the red line represents the results of this work, while the purple line represents the photon iso-effective dose model. (b) For BSH distribution: the blue line represents the results of this work, while the orange line represents the photon iso-effective dose model.

a lower probability of cell survival at the same dose. The same result is corroborated in the literature by Guerra Liberal et al.[17] Interestingly, experiments conducted by Phoenix et al. with V79 cells show an opposite conclusion,[15] likely attributable to biological differences in V79 cells or the relatively high dose of α in their experimental setup, which may limit detection sensitivity. Additionally, the α particles used in their experiments differed in energy from those produced in BNCT, which could affect the effectiveness of the synergistic effects. Moreover, their radiation exposure was conducted at 10°C, where cell repair during exposure is expected to be minimal, potentially overlooking the synergistic effects caused by the repair processes in this study. Based on the results in Figure 4b, it can be speculated that spatial differences in DSBs distribution caused by different radiation fields within the nucleus contribute to the synergistic effects. Consequently, during DSB end recombination, ends from different chromosomes may improperly join, resulting in these more lethal misrepairs.

Cell survival curves at different boron dose occupancies were also compared (Figure 7c), and it can be found that the biological effect is greater at low boron concentrations, the experimental results of Masunaga et al. and Hiratsuka et al. also have the same conclusion.[4,42] It is hypothesized that, with higher boron concentrations, the misrepair of DSBs in each affected cell becomes more complex and frequent. However, the number of cells in which DSBs are produced decreases. As a result, the overall cell survival rate appears higher at increased boron concentrations. This outcome suggests that the heterogeneity of DNA damage among cells may impact the RBE value.

In conclusion, the results show that the RBE can be predicted using this method for different radiation types as well as at macroscopic therapeutic doses in BNCT, and indicate synergistic effects between different radiation fields. This approach offers valuable insights for developing new boron drugs and accurately assessing bio-weighted doses in clinical settings. Furthermore, the method can be extended to assess RBE in other treatments.

Nonetheless, it is crucial that this research is still in its preliminary stage and requires further advancement for broader applicability. The following points outline the research limitations and directions for future development.

1. Medras cannot simulate repair mechanisms specific to individual cell lines, so the results obtained do not represent any particular cell line. The behaviors investigated in this study apply to a range of cell lines rather than a single type. While it is feasible to adjust Medras parameters to fit experimental data from various cell lines, this approach can be less informative and prone to over-fitting due to the high degree of experimental variability. Therefore, the method serves as a framework for estimating RBE, and with more experimental data, predictions for specific cell lines could be refined.
2. The dose correction factor will vary somewhat from cell model to cell model. Given the differences in nucleus size among human cells,[43] only one cell size was considered here. Variations in cell size may lead to different results, subsequent work can explore whether different cell and nucleus sizes affect the results, reflecting cell specificity to some extent.

5 | CONCLUSION

In this study, a cellular DNA damage repair model was used to predict cell survival under different radiation doses in BNCT, assessing the therapy's biological effectiveness and synergistic effects in mixed radiation fields. Additionally, the impact of varying distributions and concentrations of boron drugs on outcomes was explored. The calculated RBE and CBE values aligned with experimental results.

This method quantitatively confirmed the synergistic effects of mixed radiation fields in BNCT and the treatment's dose dependency, which are critical for evaluating therapeutic efficacy. This approach estimates biological effects by considering DNA damage distribution and subsequent cellular repair responses, enabling the generation of cell survival curves without experimental testing. Furthermore, it allows for predicting the biological effects of newly developed boron drugs, considering different boron dose occupancy ratios and boron drug distribution, thus providing a promising approach for optimizing BNCT treatment planning.

ACKNOWLEDGMENTS

This work was supported by the National Key Research and Development Program (grant number 2023YFE0197700); the National Natural Science Foundation of China (grant number 12261131621); the Natural Science Foundation of Jiangsu Province (grant number BK20220132). This work is partially supported by High Performance Computing Platform of Nanjing University of Aeronautics and Astronautics. We would like to extend our gratitude to Stephen McMahon from Queen's University Belfast for his insights and assistance with this work.

CONFLICT OF INTEREST STATEMENT

The author declares no conflicts of interest.

REFERENCES

1. Barth RF, Coderre JA, Vicente MGH, Blue TE. Boron neutron capture therapy of cancer: current status and future prospects. *Clin Cancer Res*. 2005;11(11):3987-4002. doi:10.1158/1078-0432.CCR-05-0035
2. Sato T, Masunaga SI, Kumada H, Hamada N. Microdosimetric modeling of biological effectiveness for boron neutron capture therapy considering intra- and intercellular heterogeneity in 10B distribution. *Sci Rep*. 2018;8(1):988. doi:10.1038/s41598-017-18871-0
3. Fukuda H. Response of normal tissues to boron neutron capture therapy (BNCT) with 10B-borocaptate sodium (BSH) and 10B-paraboronophenylalanine (BPA). *Cells*. 2021;10(11):2883. doi:10.3390/cells10112883
4. Hiratsuka J, Kono M, Mishima Y. RBEs of thermal neutron capture therapy and ^{10}B(n,α)^{7}Li reaction on melanoma-bearing hamsters. *Pigm Cell Res*. 1989;2(4):352-355. doi:10.1111/j.1600-0749.1989.tb00219.x
5. Coderre JA, Slatkin DN, Micca PL, Ciallella JR. Boron neutron capture therapy of a murine melanoma with p-Boronophenylalanine: dose-response analysis using a morbidity index. *Radiat Res*. 1991;128(2):177. doi:10.2307/3578135
6. Coderre JA, Makar MS, Micca PL, Nawrocky MM. Derivations of relative biological effectiveness for the high-let radiations produced during boron neutron capture irradiations of the 9l rat gliosarcoma in vitro and in vivo. *Radiat Oncol*. 1993;27(5):1121-1129.
7. Han Y, Geng C, Liu Y, et al. Calculation of the DNA damage yield and relative biological effectiveness in boron neutron capture therapy via the Monte Carlo track structure simulation. *Phys Med Biol*. 2023;68(17):175028. doi:10.1088/1361-6560/acec2a
8. Nakano H, Kawahara D, Tanabe S, et al. Calculated relative biological effectiveness (RBE) for initial DNA double-strand breaks (DSB) from flattening filter and flattening filter-free 6 MV X-ray fields. *BJR|Open*. 2021;3(1):20200072. doi:10.1259/bjro.20200072
9. Frankenberg D. Repair of DNA double-strand breaks and its effect on RBE. *Adv Space Res*. 1994;14(10):235-248. doi:10.1016/0273-1177(94)90473-1
10. Warmenhoven JW, Henthorn NT, Ingram SP, et al. Insights into the non-homologous end joining pathway and double strand break end mobility provided by mechanistic in silico modelling. *DNA Repair (Amst)*. 2020;85:102743. doi:10.1016/j.dnarep.2019.102743
11. McMahon SJ, Prise KM. A mechanistic DNA repair and survival model (Medras): applications to intrinsic radiosensitivity, relative biological effectiveness and dose-rate. *Front Oncol*. 2021;11:689112. doi:10.3389/fonc.2021.689112
12. Belov OV, Krasavin EA, Lyashko MS, Batmunkh M, Sweilam NH. A quantitative model of the major pathways for radiation-induced DNA double-strand break repair. *J Theor Biol*. 2015;366:115-130. doi:10.1016/j.jtbi.2014.09.024
13. Chatzipapas KP, Tran NH, Dordevic M, et al. Simulation of DNA damage using Geant4-DNA: an overview of the "molecularDNA" example application. *Precision Radiat Oncol*. 2023;7(1):4-14. doi:10.1002/pro6.1186
14. Maliszewska-Olejniczak K, Kaniowski D, Araszkiewicz M, Tymińska K, Korgul A. Molecular mechanisms of specific cellular DNA damage response and repair induced by the mixed radiation field during boron neutron capture therapy. *Front Oncol*. 2021;11:676575. doi:10.3389/fonc.2021.676575
15. Phoenix B, Green S, Hill MA, Jones B, Mill A, Stevens DL. Do the various radiations present in BNCT act synergistically? Cell survival experiments in mixed alpha-particle and gamma-ray fields. *Appl Radiat Isot*. 2009;67(7-8):S318-S320. doi:10.1016/j.apradiso.2009.03.097
16. Zaider M, Rossi HH. The synergistic effects of different radiations. *Radiat Res*. 1980;83(3):732. doi:10.2307/3575352
17. Guerra Liberal FDC, Thompson SJ, Prise KM, McMahon SJ. High-LET radiation induces large amounts of rapidly-repaired sublethal damage. *Sci Rep*. 2023;13(1):11198. doi:10.1038/s41598-023-38295-3
18. Deriano L, Roth DB. Modernizing the nonhomologous end-joining repertoire: alternative and classical NHEJ share the stage. *Annu Rev Genet*. 2013;47(1):433-455. doi:10.1146/annurev-genet-110711-155540
19. Krejci L, Altmannova V, Spirek M, Zhao X. Homologous recombination and its regulation. *Nucleic Acids Res*. 2012;40(13):5795-5818. doi:10.1093/nar/gks270
20. Waters CA, Strande NT, Wyatt DW, Pryor JM, Ramsden DA. Nonhomologous end joining: a good solution for bad ends. *DNA Repair (Amst)*. 2014;17:39-51. doi:10.1016/j.dnarep.2014.02.008
21. Schuemann J, McNamara AL, Warmenhoven JW, et al. A new standard DNA damage (SDD) data format. *Radiat Res*. 2018;191(1):76. doi:10.1667/RR15209.1
22. McMahon SJ. The linear quadratic model: usage, interpretation and challenges. *Phys Med Biol*. 2018;64(1):01TR01. doi:10.1088/1361-6560/aaf26a

23. Ono K, Masunaga SI, Suzuki M, Kinashi Y, Takagaki M, Akaboshi M. The combined effect of boronophenylalanine and borocaptate in boron neutron capture therapy for SCCVII tumors in mice. *Int J Radiat Oncol*Biol*Phys*. 1999;43(2):431-436. doi:10.1016/S0360-3016(98)00421-0
24. Yoshida F, Matsumura A, Shibata Y, et al. Cell cycle dependence of boron uptake from two boron compounds used for clinical neutron capture therapy. *Cancer Lett*. 2002;187(1-2):135-141. doi:10.1016/S0304-3835(02)00380-4
25. Michiue H, Sakurai Y, Kondo N, et al. The acceleration of boron neutron capture therapy using multi-linked mercaptoundecahydrododecaborate (BSH) fused cell-penetrating peptide. *Biomaterials*. 2014;35(10):3396-3405. doi:10.1016/j.biomaterials.2013.12.055
26. Incerti S, Kyriakou I, Bernal MA, et al. Geant4-DNA example applications for track structure simulations in liquid water: a report from the Geant4-DNA Project. *Med Phys*. 2018;45(8):722-739. doi:10.1002/mp.13048
27. Incerti S, Ivanchenko A, Karamitros M, et al. Comparison of GEANT4 very low energy cross section models with experimental data in water. *Med Phys*. 2010;37(9):4692-4708. doi:10.1118/1.3476457
28. Schuemann J, McNamara AL, Ramos-Méndez J, et al. TOPAS-nBio: an extension to the TOPAS simulation toolkit for cellular and sub-cellular radiobiology. *Radiat Res*. 2018;191(2):125. doi:10.1667/RR15226.1
29. González SJ, Cruz GAS. The photon-isoeffective dose in boron neutron capture therapy. *Radiat Res*. 2012;178(6):609-621. doi:10.1667/RR2944.1
30. Shiba S, Wakatsuki M, Ohno T, Nakano T. Differences in linear energy transfer affect cell-killing and radiosensitizing effects of spread-out carbon-ion beams. *Anticancer Res*. 2020;40(10):5497-5502. doi:10.21873/anticanres.14561
31. Maeda J, Cartwright IM, Haskins JS, et al. Relative biological effectiveness in canine osteosarcoma cells irradiated with accelerated charged particles. *Oncol Lett*. 2016;12(2):1597-1601. doi:10.3892/ol.2016.4808
32. McMahon SJ, Schuemann J, Paganetti H, Prise KM. Mechanistic modelling of DNA repair and cellular survival following radiation-induced DNA damage. *Sci Rep*. 2016;6(1):33290. doi:10.1038/srep33290
33. Matsuya Y, Tsutsumi K, Sasaki K, Date H. Evaluation of the cell survival curve under radiation exposure based on the kinetics of lesions in relation to dose-delivery time. *J Radiat Res (Tokyo)*. 2015;56(1):90-99. doi:10.1093/jrr/rru090
34. Flint DB, Ruff CE, Bright SJ, et al. An empirical model of proton RBE based on the linear correlation between x-ray and proton radiosensitivity. *Med Phys*. 2022;49(9):6221-6236. doi:10.1002/mp.15850
35. Thomas P, Tracy B, Ping T, et al. Relative biological effectiveness (RBE) of alpha radiation in cultured porcine aortic endothelial cells. *Int J Radiat Biol*. 2007;83(3):171-179. doi:10.1080/09553000601146915
36. Beucher A, Birraux J, Tchouandong L, et al. ATM and artemis promote homologous recombination of radiation-induced DNA double-strand breaks in G2. *EMBO J*. 2009;28(21):3413-3427. doi:10.1038/emboj.2009.276
37. Wu J, Fu Q, Quan Y, et al. Repair rates of DNA double-strand breaks under different doses of proton and γ-ray irradiation. *Nucl Instrum Methods Phys Res, Sect B*. 2012;276:1-6. doi:10.1016/j.nimb.2012.01.022
38. Ahmed EA, Vélaz E, Rosemann M, Gilbertz KP, Scherthan H. DNA repair kinetics in SCID mice Sertoli cells and DNA-PKcs-deficient mouse embryonic fibroblasts. *Chromosoma*. 2017;126(2):287-298. doi:10.1007/s00412-016-0590-9
39. Riballo E, Doherty A, Smith GCM, et al. A pathway of double-strand break rejoining dependent upon ATM, artemis, and proteins locating to gamma-H2AX foci. *Mol Cell*. 2004;16(5):715-724. doi:10.1016/j.molcel.2004.10.029
40. Oeck S, Szymonowicz K, Wiel G, et al. Relating linear energy transfer to the formation and resolution of DNA repair foci after irradiation with equal doses of X-ray photons, plateau, or Bragg-peak Protons. *Int J Mol Sci*. 2018;19(12):3779. doi:10.3390/ijms19123779
41. Suzuki M, Masunaga S, Kinashi Y, et al. The effects of boron neutron capture therapy on liver tumors and normal hepatocytes in mice. *Jpn J Cancer Res*. 2000;91(10):1058-1064. doi:10.1111/j.1349-7006.2000.tb00885.x
42. Ichiro MS, Sakurai Y, Tanaka H, et al. The dependency of compound biological effectiveness factors on the type and the concentration of administered neutron capture agents in boron neutron capture therapy. *SpringerPlus*. 2014;3(1):128. doi:10.1186/2193-1801-3-128
43. Webster M, Witkin KL, Cohen-Fix O. Sizing up the nucleus: nuclear shape, size and nuclear-envelope assembly. *J Cell Sci*. 2009;122(10):1477-1486. doi:10.1242/jcs.037333

How to cite this article: Yu C, Geng C, Tang X. Assessing the biological effects of boron neutron capture therapy through cellular DNA damage repair model. *Med Phys*. 2024;51:9372–9384. https://doi.org/10.1002/mp.17446